

Mass spectra of double-bottom baryons

Zhen-Yu Li^{1,*}, Guo-Liang Yu^{2,†}, Zhi-Gang Wang^{2,‡}, Jian-Zhong Gu³, and Hong-Tao Shen⁴

¹ School of Physics and Electronic Science,

Guizhou Education University, Guiyang 550018, China

² Department of Mathematics and Physics,

North China Electric Power University, Baoding 071003, China

³ China Institute of Atomic Energy, Beijing 102413, China

⁴ Guangxi Key Laboratory of Nuclear Physics and Technology,

Guangxi Normal University, Guilin 541006, China

(Dated: March 17, 2023)

Based on the relativistic quark model and the infinitesimally shifted Gaussian basis function method, we investigate the mass spectra of double bottom baryons systematically. In the ρ -mode which appears lower in energy than the other excited modes, we obtain the allowed quantum states and perform a systematic study of the mass spectra of the Ξ_{bb} and Ω_{bb} families. We analyze the root mean square radii and quark radial probability density distributions to deeply understand the structure of the heavy baryons. Meanwhile, the mass spectra allow us to successfully construct the Regge trajectories in the (J, M^2) plane. We also predict the masses of the ground states of double bottom baryons and discuss the differences between the structures of our spectra and those from other theoretical methods. At last, the shell structure of the double bottom baryon spectra is shown, from which one could get a bird's-eye view of the mass spectra.

Key words: Double bottom baryons, Mass spectra, Relativistic quark model.

PACS numbers: 13.25.Ft; 14.40.Lb

I. Introduction

The spectroscopy of doubly heavy baryons contains rich information of strong interactions and has become one of the hot topics in hadronic physics. In the past decades, research on the doubly heavy baryons has developed rapidly in both experiments and theories. The SELEX collaboration first reported the observation of the Ξ_{cc}^+ baryon in 2002 [1]. But the confirmation of the Ξ_{cc}^+ baryon was not yet completed and searching for the doubly heavy baryons came to a standstill. Recently, the Ξ_{cc}^{++} baryon was observed by the LHCb collaboration [2–4] and has been collected in the new PDG

*Electronic address: zhenyvli@163.com

†Electronic address: yuguoliang2011@163.com

‡Electronic address: zgwang@aliyun.com

data [5], which is an important progress in the study of doubly heavy baryons. The efforts of searching for Ξ_{bc}^0 [6], Ω_{bc}^0 [7] and Ξ_{bc}^+ [8] baryons were reported one after another later on. Although the Ξ_{bb} or Ω_{bb} has not been found experimentally, they are expected to be observed in the near future [9, 10].

On the other hand, the progress in experiment stimulates the theoretical studies on the spectroscopy of doubly heavy baryons, including the non-relativistic quark model [11], the effective field theory [12], the chiral perturbation theory [13], the MIT bag model [14], the effective QCD string theory [15], the QCD sum rules [16–18], the Bethe-Salpeter equation approach [19, 20], the di-quark picture in a relativized quark model [21], the hyper-central constituent quark model [22–24], the lattice QCD [25], the chiral partner structure method [26], and the Regge phenomenology [27]. The theoretical studies mentioned above help us to understand the structure of double heavy baryons.

Nevertheless, the theoretical predictions with different methods vary widely, probably being lack of experimental data. Table I lists the predicted masses of the ground states of double bottom baryons from different theoretical methods in the past three decades. As shown in Table I, the predicted masses of the ground states for the Ξ_{bb} baryons range from 9800 MeV to 10340 MeV, and the maximal difference amounts to 540 MeV. In addition, there are problems in theory which need to be studied. For example, the structure of the mass spectra is not clear so far. So, it would be helpful to analyze the mass spectra of heavy baryons in a systematic way. Some theoretical efforts have been made indeed to solve these problems in this way [11, 15, 21–24, 28–30].

In our previous papers [31, 32], we have analyzed the mass spectra of singly heavy baryons systematically, by using the relativistic quark model [33, 34] and the infinitesimally shifted Gaussian(ISG) function method [35]. For singly heavy baryons, the excited state is confined to the λ -mode, which has a lower energy than the other modes. It turns out that most of the mass observed in the experiment can be reproduced well using our calculations. Because the λ -mode is associated with the heavy quark, it seems that heavy baryon excitation may be dominated by the excitation of heavy quarks in the heavy quark limit. If this conjecture holds, the excitation of the double heavy baryons should be dominated by the excitation of the two heavy quarks. According to this idea, in this paper, we will try to systematically analyze the mass spectra of double-bottom baryons, and further understand the structure of heavy baryons.

This paper is organized as follows. In Sect.II, we briefly describe the methods used in the theoretical calculations; In Sect.III, we present the root mean square radii and the mass spectra of the doubly bottom baryons, analyze their quark radial probability density distributions, construct the Regge trajectories, and explore the spectral shell structure; And Sect.IV is reserved for our conclusions.

TABLE I: Predicted masses (in MeV) of the ground states of the double bottom baryons in the references. The superscript * refers to the $J = 3/2$ baryons.

$m(\Xi_{bb})$	$m(\Xi_{bb}^*)$	$m(\Omega_{bb})$	$m(\Omega_{bb}^*)$	year	$m(\Xi_{bb})$	$m(\Xi_{bb}^*)$	$m(\Omega_{bb})$	$m(\Omega_{bb}^*)$	year
10322	10355	10500	10533	2022 [11]	10143	10178	10273	10308	2014 [43]
10221	10261	-	-	2022 [24]	10162	10184	-	-	2014 [44]
10171	10195	10266	10291	2022 [29]	10322	10352	-	-	2012 [45]
10235	-	10299	-	2021 [13]	9800	9890	9890	9930	2012 [46]
10311	10360	10408	10451	2021 [14]	10090	-	10185	-	2011 [47]
10120	10150	-	-	2021 [15]	10170	10220	10320	10380	2010 [48]
10230	10333	10350	10449	2021 [36]	10185	10216	10271	10289	2009 [49]
10210	10221	10319	10331	2020 [37]	10202	10237	10359	10389	2008 [50]
10091	10103	10190	10203	2020 [38]	10189	10218	10293	10321	2008 [51]
10182	10214	10276	10309	2019 [19]	10340	10367	10454	10486	2008 [52]
10169	10189	10259	10268	2018 [39]	10130	10144	10422	10432	2008 [53]
-	-	10208	-	2018 [40]	9780	10350	9850	10280	2008 [54]
10220	10270	10330	10370	2018 [16]	10062	10101	10208	10244	2008 [55]
10250	10270	10340	10350	2018 [20]	10197	10236	10260	10297	2007 [56]
10317	10340	-	-	2017 [22]	10100	10110	10280	10290	2004 [57]
10138	10169	10230	10258	2017 [21]	10202	10236	10359	10389	2002 [28]
-	-	10446	10467	2016 [23]	10090	10110	10210	10260	2002 [58]
10199	10316	10320	10431	2015 [27]	10093	10133	10180	10200	2000 [59]
10314	10339	10447	10467	2015 [30]	10230	10280	10320	10360	1997 [60]
10267	-	10356	-	2015 [41]	10198	10236	-	-	1996 [61]
10334	10431	10397	10495	2014 [42]	10340	10370	10370	10400	1995 [62]

II. Phenomenological methods adopted in this work

In this work, we use the relativistic quark model and the ISG method to study double bottom baryons. The detailed discussions about these two methods can be found in references [31–35]. The doubly heavy baryon is a three-quark system, which is commonly studied in the Jacobi coordinates. As shown in Fig.1, there are three channels of the Jacobi coordinates for the three-quark system. The corresponding Jacobi coordinates are defined as

$$\boldsymbol{\rho}_i = \mathbf{r}_j - \mathbf{r}_k, \quad (1)$$

$$\boldsymbol{\lambda}_i = \mathbf{r}_i - \frac{m_j \mathbf{r}_j + m_k \mathbf{r}_k}{m_j + m_k}, \quad (2)$$

where $i, j, k = 1, 2, 3$ (or replace their positions in turn). \mathbf{r}_i and m_i denote the position vector and the mass of the i th quark, respectively.

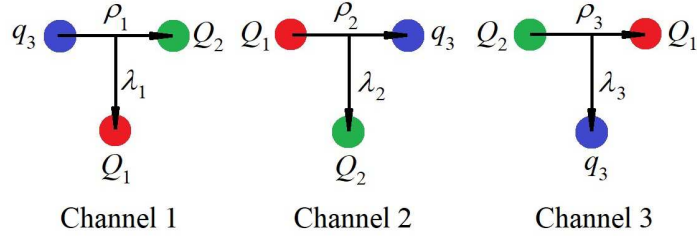


FIG. 1: (Color online) Jacobi coordinates for the three-body system. We denote the light quark as the 3rd particle in the case of doubly heavy baryons.

A double bottom baryon is commonly considered as a system composed of a heavy di-quark and a light quark [19, 21, 63]. Accordingly, the calculations in this work are based on channel 3. In this case, the 3rd quark is just the light quark. $\mathbf{l}_{\rho 3}$ (denoted in short as \mathbf{l}_{ρ}) is defined as the orbital angular momentum between the two bottom quarks, and $\mathbf{l}_{\lambda 3}$ (denoted in short as \mathbf{l}_{λ}) represents the one between the bottom-quark pair and the light quark.

For a definite state in theory, the spatial wave function and the spin function are written as follow,

$$|l_{\rho} l_{\lambda} L s j J M_J\rangle = \{[(|l_{\rho} m_{\rho}\rangle |l_{\lambda} m_{\lambda}\rangle)_L \times (|s_1 m_{s_1}\rangle |s_2 m_{s_2}\rangle)_{s_j}] \times |s_3 m_{s_3}\rangle\}_{JM_J}. \quad (3)$$

l_{ρ} , l_{λ} , L , s , j , J and M_J are quantum numbers which characterize a given state. Because the total wave function must be antisymmetric and the flavor function of the double bottom quark subsystem (bb) is symmetric, the total spin s and orbital quantum number l_{ρ} of (bb) should meet the condition $(-1)^{s+l_{\rho}} = -1$.

III. Numerical results and discussions

3.1 ρ -mode

$nL(J^P)$ is usually used to describe a baryon state in experiment, where the orbital quantum numbers \mathbf{l}_{ρ} and \mathbf{l}_{λ} are unmeasurable. For $L \neq 0$, there usually exist three (l_{ρ}, l_{λ}) modes under the condition $\mathbf{L} = \mathbf{l}_{\rho} + \mathbf{l}_{\lambda}$: (1) The ρ -mode with $l_{\rho} \neq 0$ and $l_{\lambda} = 0$; (2) The λ -mode with $l_{\rho} = 0$ and $l_{\lambda} \neq 0$; (3) The λ - ρ mixing mode with $l_{\rho} \neq 0$ and $l_{\lambda} \neq 0$. These (l_{ρ}, l_{λ}) modes should generally be mixed.

We first investigate the excitation energy for different modes. As an example, the excitation energies of the $1D(\frac{3}{2}^+, \frac{5}{2}^+)_{j=2}$ states as functions of m_Q are investigated. As shown in Fig.2, the excitation energies of three modes are crossed in the range of 0.2-0.9 GeV, where the heavy quark limit is invalid and the mixing between these modes can not be neglected. However, they are separated when m_Q

increases from 0.9 GeV to 5.0 GeV. And the ρ -mode appears lower in energy than the other two modes in the heavy quark limit for double bottom baryons, which is different from that of the singly heavy baryons [31, 32]. This confirms the conjecture mentioned in the introduction that the heavy quark excitation is dominant. As a reasonable approximation, we only study the ρ -mode in this work.

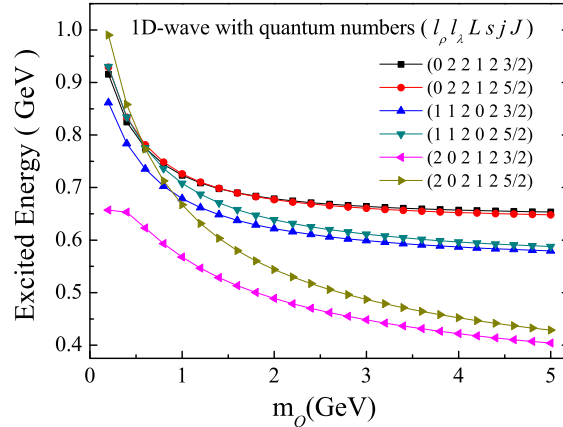


FIG. 2: (Color online) The dependence of excitation energies on m_Q for different modes of Ξ_{QQ} , where $m_1 = m_2 = m_Q$ and $m_3 = m_{u(d)}$. The excitation energies are measured from the ground state with quantum numbers $(l_\rho \ l_\lambda \ L \ s \ j \ J) = (0 \ 0 \ 0 \ 1 \ 1 \ 1/2)$.

3.2 Mass spectra, root mean square radii and quark radial probability density distributions

In the ρ mode, the root mean square radii, quark radial probability density distributions and mass spectra of the double bottom baryons with quantum numbers up to $n = 4$ and $L = 4$ are presented in Tables II-III and Figs.3-4.

Through the analysis of these calculated results, some general features of the mass spectra are summarized as follows: (1) There are a total of 18 quantum states with $L \leq 4$ in the Ξ_{bb} or Ω_{bb} family. (2) For the same L , the mass splitting becomes larger with the increase of j . For example, Table I shows the mass differences (splittings) of the 1D doublets with $j = 1, 2, 3$ are 15 MeV, 25 MeV and 35 MeV, respectively. This is apparently different from that of the singly heavy baryons [31, 32]. (3) The mass difference between the two adjacent radial excited states gradually decreases with increasing n .

On the other hand, the calculated root mean square radii and quark radial probability density distributions carry important information. For a three-quark system, the radial probability densities

$\omega(r_\rho)$ and $\omega(r_\lambda)$ can be defined as follows,

$$\begin{aligned}\omega(r_\rho) &= \int |\Psi(\mathbf{r}_\rho, \mathbf{r}_\lambda)|^2 d\mathbf{r}_\lambda d\Omega_\rho, \\ \omega(r_\lambda) &= \int |\Psi(\mathbf{r}_\rho, \mathbf{r}_\lambda)|^2 d\mathbf{r}_\rho d\Omega_\lambda,\end{aligned}\quad (4)$$

where Ω_ρ and Ω_λ are the solid angles spanned by vectors \mathbf{r}_ρ and \mathbf{r}_λ , respectively. From Figs.3-4 and Tables II-III, one can find some interesting properties. (1) For a ground state, the $\langle r_\rho^2 \rangle^{1/2}$ value is much smaller than the $\langle r_\lambda^2 \rangle^{1/2}$ value. This indicates that the two bottom quarks are bonded very tightly. (2) As shown by the two types of the root mean square radii in Table II, the main radial excitation happens in the r_ρ and r_λ spaces in turn with $n = 2, 3, 4$. This feature can be also seen in the quark radial probability density distributions in Figs.3-4. (3) As shown in Tables.II-III, for the orbital excited states with fixed n , the difference of their $\langle r_\lambda^2 \rangle^{1/2}$ values is relatively small. While their $\langle r_\rho^2 \rangle^{1/2}$ values become larger with increasing L . In Figs.3 and 4, the radial probability density distribution of $r_\lambda^2 \omega(r_\lambda)$ (dash lines) changes a little with different L values. But, the peak of the $r_\rho^2 \omega(r_\rho)$ (solid lines) is significantly shifted outward with increasing L . (4) The shapes of the black (solid) lines in Fig.3 are almost as same as those in Fig.4. And, for the same state, the $\langle r_\rho^2 \rangle^{1/2}$ value in the Ξ_{bb} family is almost the same as that in the Ω_{bb} family. This reflects the similarity in structure of the Ξ_{bb} and Ω_{bb} baryons.

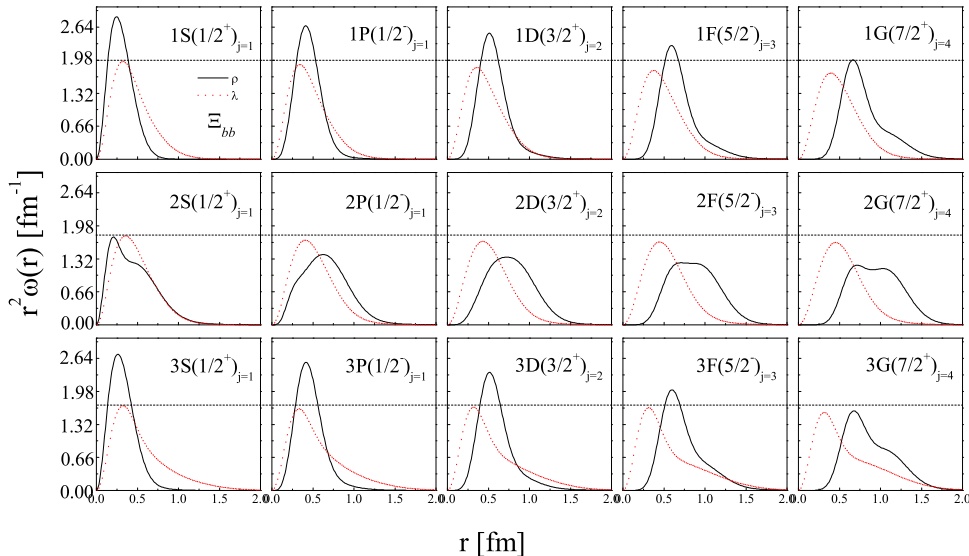


FIG. 3: (Color online) Radial probability density distributions for some nL states of the Ξ_{bb} family. The solid line denotes the probability density with r_ρ , and the dash line denotes the one with r_λ .

TABLE II: The root mean square radii (fm) and mass spectra (MeV) of the Ξ_{bb} family.

l_ρ	l_λ	L	s	j	$nL(J^P)$	$\langle r_\rho^2 \rangle^{1/2}$	$\langle r_\lambda^2 \rangle^{1/2}$	mass	l_ρ	l_λ	L	s	j	$nL(J^P)$	$\langle r_\rho^2 \rangle^{1/2}$	$\langle r_\lambda^2 \rangle^{1/2}$	mass
0 0 0 1 1					$1S(\frac{1}{2}^+)$	0.297	0.469	10192	2 0 2 1 3					$1D(\frac{7}{2}^+)$	0.596	0.540	10629
					$2S(\frac{1}{2}^+)$	0.585	0.522	10536						$2D(\frac{7}{2}^+)$	0.893	0.595	10863
					$3S(\frac{1}{2}^+)$	0.312	0.839	10686						$3D(\frac{7}{2}^+)$	0.619	0.899	11094
					$4S(\frac{1}{2}^+)$	0.757	0.555	10796						$4D(\frac{7}{2}^+)$	0.999	0.617	11159
0 0 0 1 1					$1S(\frac{3}{2}^+)$	0.299	0.483	10211	3 0 3 0 3					$1F(\frac{5}{2}^-)$	0.702	0.534	10741
					$2S(\frac{3}{2}^+)$	0.589	0.534	10552						$2F(\frac{5}{2}^-)$	0.997	0.589	10955
					$3S(\frac{3}{2}^+)$	0.312	0.847	10696						$3F(\frac{5}{2}^-)$	0.737	0.901	11211
					$4S(\frac{3}{2}^+)$	0.760	0.566	10810						$4F(\frac{5}{2}^-)$	1.253	0.648	11295
1 0 1 0 1					$1P(\frac{1}{2}^-)$	0.456	0.496	10428	3 0 3 0 3					$1F(\frac{7}{2}^-)$	0.711	0.562	10773
					$2P(\frac{1}{2}^-)$	0.746	0.550	10701						$2F(\frac{7}{2}^-)$	0.996	0.614	10981
					$3P(\frac{1}{2}^-)$	0.486	0.857	10912						$3F(\frac{7}{2}^-)$	0.740	0.923	11231
					$4P(\frac{1}{2}^-)$	0.809	0.574	10959						$4F(\frac{7}{2}^-)$	1.346	0.687	11322
1 0 1 0 1					$1P(\frac{3}{2}^-)$	0.459	0.508	10445	4 0 4 1 3					$1G(\frac{5}{2}^+)$	0.812	0.555	10876
					$2P(\frac{3}{2}^-)$	0.750	0.561	10715						$2G(\frac{5}{2}^+)$	1.078	0.604	11067
					$3P(\frac{3}{2}^-)$	0.484	0.867	10922						$3G(\frac{5}{2}^+)$	0.861	0.923	11336
					$4P(\frac{3}{2}^-)$	0.818	0.583	10973						$4G(\frac{5}{2}^+)$	1.653	0.742	11441
2 0 2 1 1					$1D(\frac{1}{2}^+)$	0.584	0.519	10600	4 0 4 1 3					$1G(\frac{7}{2}^+)$	0.824	0.582	10905
					$2D(\frac{1}{2}^+)$	0.886	0.576	10839						$2G(\frac{7}{2}^+)$	1.073	0.627	11092
					$3D(\frac{1}{2}^+)$	0.614	0.880	11074						$3G(\frac{7}{2}^+)$	0.865	0.945	11356
					$4D(\frac{1}{2}^+)$	0.921	0.592	11127						$4G(\frac{7}{2}^+)$	1.709	0.769	11461
2 0 2 1 1					$1D(\frac{3}{2}^+)$	0.587	0.531	10615	4 0 4 1 4					$1G(\frac{7}{2}^+)$	0.812	0.551	10872
					$2D(\frac{3}{2}^+)$	0.888	0.587	10851						$2G(\frac{7}{2}^+)$	1.078	0.600	11063
					$3D(\frac{3}{2}^+)$	0.614	0.890	11084						$3G(\frac{7}{2}^+)$	0.862	0.921	11334
					$4D(\frac{3}{2}^+)$	0.943	0.603	11141						$4G(\frac{7}{2}^+)$	1.655	0.740	11439
2 0 2 1 2					$1D(\frac{3}{2}^+)$	0.585	0.516	10596	4 0 4 1 4					$1G(\frac{9}{2}^+)$	0.827	0.586	10909
					$2D(\frac{3}{2}^+)$	0.887	0.572	10836						$2G(\frac{9}{2}^+)$	1.071	0.630	11096
					$3D(\frac{3}{2}^+)$	0.616	0.878	11072						$3G(\frac{9}{2}^+)$	0.867	0.948	11359
					$4D(\frac{3}{2}^+)$	0.927	0.590	11126						$4G(\frac{9}{2}^+)$	1.723	0.773	11464
2 0 2 1 2					$1D(\frac{5}{2}^+)$	0.591	0.536	10621	4 0 4 1 5					$1G(\frac{9}{2}^+)$	0.813	0.547	10868
					$2D(\frac{5}{2}^+)$	0.890	0.591	10856						$2G(\frac{9}{2}^+)$	1.078	0.597	11060
					$3D(\frac{5}{2}^+)$	0.615	0.894	11088						$3G(\frac{9}{2}^+)$	0.865	0.918	11331
					$4D(\frac{5}{2}^+)$	0.964	0.609	11149						$4G(\frac{9}{2}^+)$	1.663	0.738	11436
2 0 2 1 3					$1D(\frac{5}{2}^+)$	0.588	0.512	10594	4 0 4 1 5					$1G(\frac{11}{2}^+)$	0.831	0.590	10914
					$2D(\frac{5}{2}^+)$	0.889	0.569	10834						$2G(\frac{11}{2}^+)$	1.070	0.633	11100
					$3D(\frac{5}{2}^+)$	0.619	0.876	11072						$3G(\frac{11}{2}^+)$	0.871	0.952	11363
					$4D(\frac{5}{2}^+)$	0.942	0.588	11127						$4G(\frac{11}{2}^+)$	1.741	0.777	11467

TABLE III: The root mean square radii (fm) and mass spectra (MeV) of the Ω_{bb} family.

l_ρ	l_λ	L	s	j	$nL(J^P)$	$\langle r_\rho^2 \rangle^{1/2}$	$\langle r_\lambda^2 \rangle^{1/2}$	mass	l_ρ	l_λ	L	s	j	$nL(J^P)$	$\langle r_\rho^2 \rangle^{1/2}$	$\langle r_\lambda^2 \rangle^{1/2}$	mass
0 0 0 1 1					$1S(\frac{1}{2}^+)$	0.293	0.426	10285	2 0 2 1 3					$1D(\frac{7}{2}^+)$	0.587	0.496	10731
					$2S(\frac{1}{2}^+)$	0.573	0.483	10638						$2D(\frac{7}{2}^+)$	0.887	0.552	10972
					$3S(\frac{1}{2}^+)$	0.314	0.782	10777						$3D(\frac{7}{2}^+)$	0.615	0.844	11190
					$4S(\frac{1}{2}^+)$	0.750	0.517	10902						$4D(\frac{7}{2}^+)$	0.923	0.568	11264
0 0 0 1 1					$1S(\frac{3}{2}^+)$	0.294	0.438	10303	3 0 3 0 3					$1F(\frac{5}{2}^-)$	0.691	0.494	10851
					$2S(\frac{3}{2}^+)$	0.577	0.493	10653						$2F(\frac{5}{2}^-)$	0.997	0.551	11071
					$3S(\frac{3}{2}^+)$	0.314	0.790	10787						$3F(\frac{5}{2}^-)$	0.732	0.847	11310
					$4S(\frac{3}{2}^+)$	0.752	0.526	10915						$4F(\frac{5}{2}^-)$	1.114	0.601	11407
1 0 1 0 1					$1P(\frac{1}{2}^-)$	0.449	0.454	10528	3 0 3 0 3					$1F(\frac{7}{2}^-)$	0.700	0.517	10879
					$2P(\frac{1}{2}^-)$	0.734	0.509	10809						$2F(\frac{7}{2}^-)$	0.997	0.572	11094
					$3P(\frac{1}{2}^-)$	0.483	0.803	11007						$3F(\frac{7}{2}^-)$	0.735	0.868	11329
					$4P(\frac{1}{2}^-)$	0.792	0.533	11064						$4F(\frac{7}{2}^-)$	1.198	0.636	11432
1 0 1 0 1					$1P(\frac{3}{2}^-)$	0.451	0.465	10543	4 0 4 1 3					$1G(\frac{5}{2}^+)$	0.799	0.514	10990
					$2P(\frac{3}{2}^-)$	0.738	0.519	10821						$2G(\frac{5}{2}^+)$	1.083	0.566	11186
					$3P(\frac{3}{2}^-)$	0.482	0.813	11016						$3G(\frac{5}{2}^+)$	0.854	0.870	11437
					$4P(\frac{3}{2}^-)$	0.797	0.541	11077						$4G(\frac{5}{2}^+)$	1.456	0.728	11560
2 0 2 1 1					$1D(\frac{1}{2}^+)$	0.575	0.478	10704	4 0 4 1 3					$1G(\frac{7}{2}^+)$	0.809	0.537	11014
					$2D(\frac{1}{2}^+)$	0.879	0.535	10951						$2G(\frac{7}{2}^+)$	1.079	0.586	11207
					$3D(\frac{1}{2}^+)$	0.609	0.826	11171						$3G(\frac{7}{2}^+)$	0.858	0.890	11455
					$4D(\frac{1}{2}^+)$	0.865	0.548	11233						$4G(\frac{7}{2}^+)$	1.530	0.751	11580
2 0 2 1 1					$1D(\frac{3}{2}^+)$	0.578	0.489	10718	4 0 4 1 4					$1G(\frac{7}{2}^+)$	0.799	0.511	10986
					$2D(\frac{3}{2}^+)$	0.881	0.545	10962						$2G(\frac{7}{2}^+)$	1.083	0.563	11183
					$3D(\frac{3}{2}^+)$	0.609	0.836	11180						$3G(\frac{7}{2}^+)$	0.856	0.867	11434
					$4D(\frac{3}{2}^+)$	0.881	0.558	11246						$4G(\frac{7}{2}^+)$	1.457	0.726	11558
2 0 2 1 2					$1D(\frac{3}{2}^+)$	0.576	0.475	10702	4 0 4 1 4					$1G(\frac{9}{2}^+)$	0.812	0.541	11018
					$2D(\frac{3}{2}^+)$	0.880	0.533	10948						$2G(\frac{9}{2}^+)$	1.078	0.588	11210
					$3D(\frac{3}{2}^+)$	0.611	0.824	11170						$3G(\frac{9}{2}^+)$	0.861	0.893	11457
					$4D(\frac{3}{2}^+)$	0.869	0.546	11232						$4G(\frac{9}{2}^+)$	1.550	0.755	11582
2 0 2 1 2					$1D(\frac{5}{2}^+)$	0.582	0.492	10724	4 0 4 1 5					$1G(\frac{9}{2}^+)$	0.800	0.508	10983
					$2D(\frac{5}{2}^+)$	0.884	0.548	10966						$2G(\frac{9}{2}^+)$	1.083	0.560	11180
					$3D(\frac{5}{2}^+)$	0.611	0.839	11184						$3G(\frac{9}{2}^+)$	0.858	0.865	11432
					$4D(\frac{5}{2}^+)$	0.896	0.562	11253						$4G(\frac{9}{2}^+)$	1.466	0.726	11557
2 0 2 1 3					$1D(\frac{5}{2}^+)$	0.579	0.472	10700	4 0 4 1 5					$1G(\frac{11}{2}^+)$	0.816	0.544	11022
					$2D(\frac{5}{2}^+)$	0.883	0.530	10947						$2G(\frac{11}{2}^+)$	1.076	0.591	11213
					$3D(\frac{5}{2}^+)$	0.615	0.822	11170						$3G(\frac{11}{2}^+)$	0.865	0.897	11461
					$4D(\frac{5}{2}^+)$	0.881	0.545	11235						$4G(\frac{11}{2}^+)$	1.576	0.759	11586

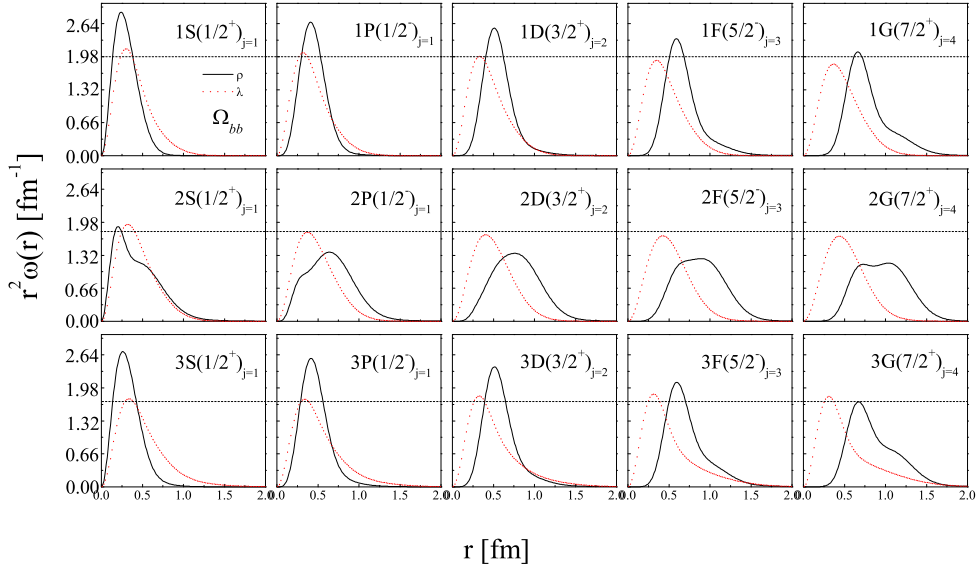


FIG. 4: (Color online) Same as Fig.3, but for the Ω_{bb} family.

3.3 Regge trajectories

For singly heavy baryons, we have successfully constructed the Regge trajectories[31, 32, 64–67], where the mass spectra were obtained in the λ -mode. In this work, we study the Regge trajectories of double bottom baryons in the ρ -mode. We use the following definition for the (J, M^2) Regge trajectories,

$$M^2 = \alpha J + \beta, \quad (5)$$

where α and β are the slope and intercept. In Figs.5-6, we plot the Regge trajectories in the (J, M^2) plane with our calculated mass spectra. The four lines in each figure correspond to the radial quantum number $n = 1, 2, 3, 4$, respectively. The fitted slopes and intercepts of the Regge trajectories are given in Table IV.

As shown in Fig.5, the group with natural parity (NP) $(-1)^{J-1/2}$ is composed of $S(\frac{1}{2}^+)_{j=1}$, $P(\frac{3}{2}^-)_{j=1}$, $D(\frac{5}{2}^+)_{j=2}$, $F(\frac{7}{2}^-)_{j=3}$ and $G(\frac{9}{2}^+)_{j=4}$ states. The group with the unnatural parity (UP) $(-1)^{J+1/2}$ is composed of $P(\frac{1}{2}^-)_{j=1}$, $D(\frac{3}{2}^+)_{j=2}$, $F(\frac{5}{2}^-)_{j=3}$ and $G(\frac{7}{2}^+)_{j=4}$ states. In fact, there are 18 members of the Ξ_{bb} family in this work. The remaining 9 states can also be put into these lines, because their mass values are very near those states with the same $L(J^P)$. The situation is similar for the Ω_{bb} family as shown in Fig.6.

It is shown that the linear trajectories appear clearly in the (J, M^2) plane. Most of the data points fall on the trajectory lines. This indicates that the Regge trajectories have a strong universality. However, these lines are in whole not equidistant, which is different from those in references [22–24].

On the other hand, the linear trajectories in the (n, M^2) plane can not be constructed from our predicted masses, the reason is similar to that of the singly heavy baryons [31, 32]. But, the linear Regge trajectories in the (n, M^2) plane for double bottom baryons are obtained within a hyper-central constituent quark model [23]. If the experiment in the near future touches the sub-shells of $n = 3$ and 4, it might be a good time to check the (n, M^2) Regge trajectories.

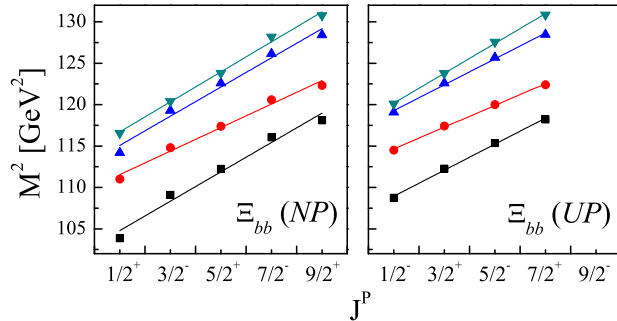


FIG. 5: (Color online) (J, M^2) Regge trajectories for the Ξ_{bb} family and M^2 is in GeV^2 . The NP denotes the natural parity, and the UP denotes the unnatural parity.

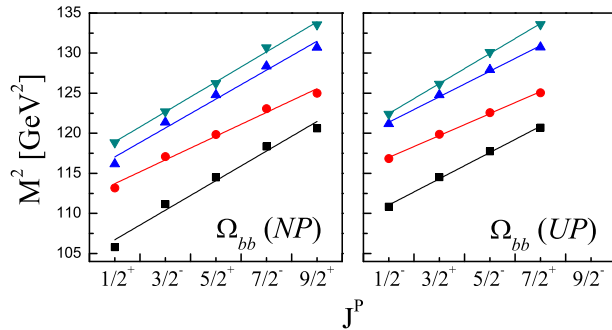


FIG. 6: (Color online) Same as Fig. 5, but for the Ω_{bb} family.

3.4 Shell structure of the mass spectra

To get a clear outline of the baryon spectra, the shell structures of the mass spectra of Ξ_{bb} and Ω_{bb} baryons are presented respectively. As shown in Figs. 7 and 8, there lies a big gap (about 230 MeV)

TABLE IV: Fitted values of the slope and intercept of the Regge trajectories for the Ξ_c and Ξ'_c families.

Trajectory	Ξ_{bb}		Ω_{bb}	
	$\alpha(\text{GeV}^2)$	$\beta(\text{GeV}^2)$	$\alpha(\text{GeV}^2)$	$\beta(\text{GeV}^2)$
$n = 1(NP)$	3.547 ± 0.301	103.003 ± 0.864	3.689 ± 0.296	104.859 ± 0.851
$n = 2(NP)$	2.840 ± 0.191	110.119 ± 0.550	2.963 ± 0.188	112.225 ± 0.541
$n = 3(NP)$	3.525 ± 0.278	113.308 ± 0.800	3.609 ± 0.283	115.238 ± 0.813
$n = 4(NP)$	3.624 ± 0.141	114.889 ± 0.405	3.741 ± 0.121	117.054 ± 0.348
$n = 1(UP)$	3.147 ± 0.112	107.354 ± 0.255	3.277 ± 0.119	109.398 ± 0.273
$n = 2(UP)$	2.623 ± 0.084	113.337 ± 0.193	2.738 ± 0.084	115.603 ± 0.193
$n = 3(UP)$	3.126 ± 0.118	117.700 ± 0.270	3.189 ± 0.126	119.765 ± 0.289
$n = 4(UP)$	3.604 ± 0.079	118.370 ± 0.180	3.749 ± 0.067	120.571 ± 0.153

between the $1S$ and $1P$ sub-shells. This implies the experimental measurement of the $1S$ states for the Ξ_{bb} or Ω_{bb} baryons could be done cleanly.

For each ground state, we average the predicted masses including ours and those listed in Table I, and compute the deviations (errors) from the mean value. The errors for different ground states are displayed in Fig.9. The mean values are obtained with $\bar{m} = \sum_{i=1}^N m_i/N$. The errors are calculated with $\Delta m_i = m_i - \bar{m}$ and listed in chronological order. There are a total of 43 theoretical results here. The obtained mean masses are as follows: $\bar{m}_{th}(\Xi_{bb})=10183$ MeV, $\bar{m}_{th}(\Xi'_{bb})=10234$ MeV, $\bar{m}_{th}(\Omega_{bb})=10287$ MeV and $\bar{m}_{th}(\Omega'_{bb})=10337$ MeV.

As mentioned in section I, references [11, 15, 21–24, 28–30] have studied the mass spectral structures. We compare our mass spectral structures with those of references [24] and [28]. As shown in Table V, one can see the predicted masses of the S states from the two references and ours are generally consistent with each other. Nevertheless, the difference between them starts with the P states. In our calculations, there are only two P states due to the limitation of the ρ -mode. But, references [28] and [24] predict more P states than ours. In Table V, we list some predicted mass values of the P states from references [28] and [24], and label them in the way of $nL(J^P)$. For these P states, the masses from the reference [28] are smaller than those from the reference [24] and ours as a whole. In addition, for the reference [24], the predicted masses of the $P(\frac{1}{2}^-)$ states are greater than those of the $P(\frac{3}{2}^-)$ states, and the mass splittings of the P doublets are rather small. In general, the mass spectral structures given by the three papers are different.

In fact, it can be seen that different theoretical models speculate different inner structures of baryons and lead to different results. This reflects the complexity of theoretical calculation for doubly heavy baryons. We look forward to experimental testing of these models and further understanding of the structure of double bottom baryons.

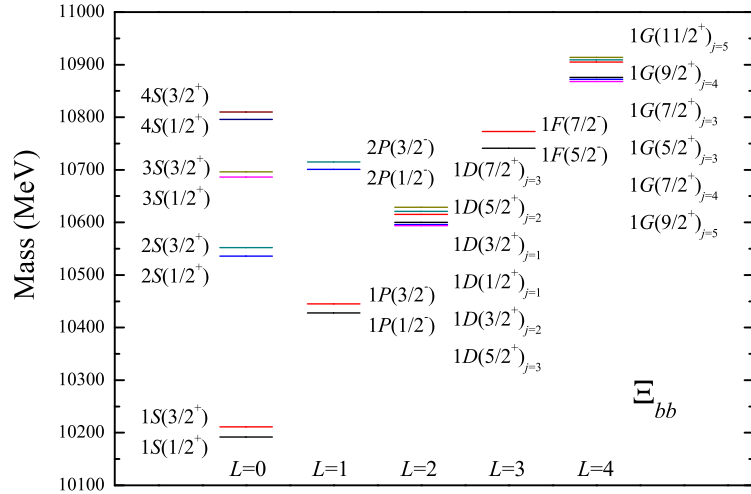


FIG. 7: (Color online) Shell structure of the Ξ_{bb} family. The mass is measured in MeV.

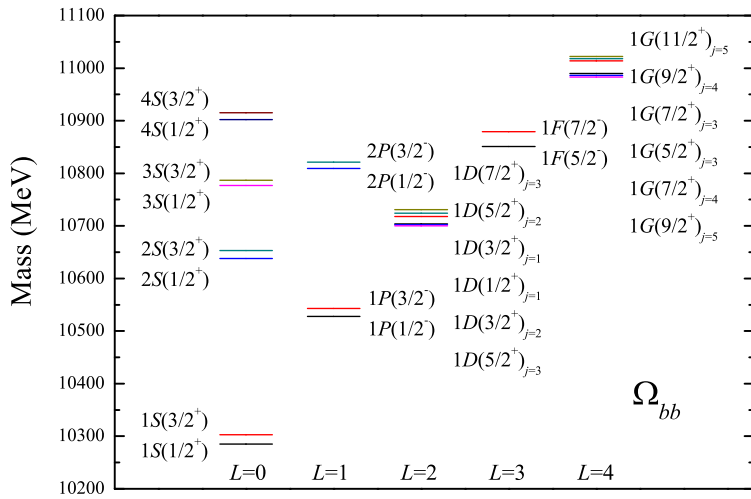


FIG. 8: (Color online) Same as Fig.7, but for the Ω_{bb} family.

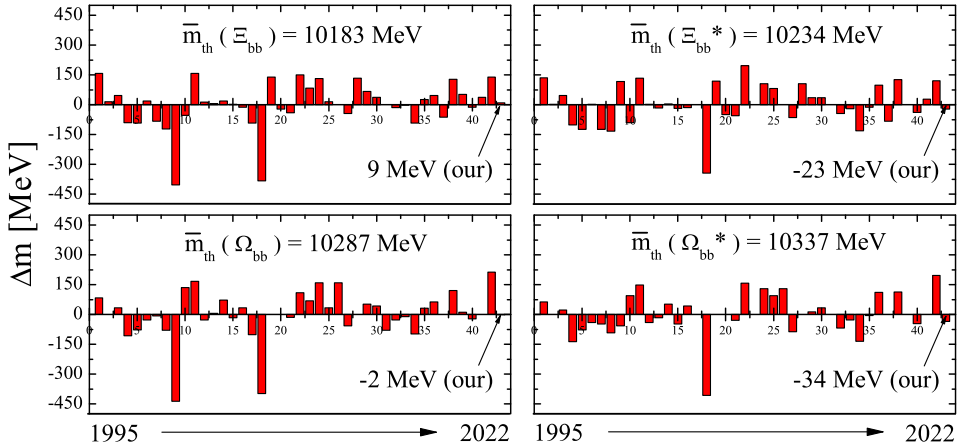


FIG. 9: (Color online) Mass errors from the mean masses of the theoretical calculated masses of the ground states for double bottom baryons given by the references in recent 30 years. The mass errors in this work are indicated. The mean masses are also presented.

TABLE V: The masses (MeV) of the S and P states for Ξ_{bb} baryons.

	$n = 1$	$n = 2$	$n = 3$	$n = 4$	$n = 1$	$n = 2$	$n = 3$	$n = 4$	
$L(J^P)$	$S(\frac{1}{2}^+)$					$S(\frac{3}{2}^+)$			
[28]	10202	10441	10630	10832	10237	10482	10673	10860	
[24]	10221	10525	10749	10940	10261	10540	10756	10943	
our	10192	10536	10686	10796	10211	10552	10696	10810	
$L(J^P)$	$P(\frac{1}{2}^-)$					$P(\frac{3}{2}^-)$			
[28]	10368	10563	10632	10744	10408	10607	10673	10788	
[24]	10458	10686	10883	11055	10456	10685	10882	11055	
our	10428	10701	10912	10959	10445	10715	10922	10973	

IV. Conclusions

In this work, combining the relativistic quark model with the ISG method, we investigate the double bottom baryon spectra systematically. The calculated result shows that the ρ -mode appears lower in energy than the other modes, which confirms the conjecture of the heavy quark excitation domination for the singly- and doubly-heavy baryons. Consequently, as a reasonable approximation, we obtain the mass spectra of the Ξ_{bb} and Ω_{bb} families in the ρ -mode. We also investigate the root mean square radii and the quark radial probability density distributions of these states, which deepens the understanding

of the structure of double bottom baryons.

Based on the predicted mass spectra, we construct successfully the Regge trajectories in the (J, M^2) plane. These trajectories are not parallel to each other and not equidistant as a whole. Nevertheless, we can not currently construct the linear trajectories in the (n, M^2) plane, which is an apparent difference between our mass spectra and those obtained from some other models.

At last, the mass spectral structures of the Ξ_{bb} and Ω_{bb} families are presented, from which we could get a bird's-eye view of the mass spectra. Then, we discuss the masses of the ground states of double bottom baryons and examine the reliability of our mass prediction through an extensive comparison with those given by the theoretical studies in the past three decades. We also analyze the differences between the structures of our spectra and those from other theoretical methods.

This work is a continuation of the series of our studies on the heavy baryons. The calculations in this work are systematic and the predicted masses and mass spectral structures might be a useful reference for related experiments.

Acknowledgements

This research is supported by the Central Government Guidance Funds for Local Scientific and Technological Development of China (No. Guike ZY22096024), the National Natural Science Foundation of China (Grant No. 11675265), the Continuous Basic Scientific Research Project (Grant No. WDJC-2019-13), and the Leading Innovation Project (Grant No. LC 192209000701).

- [1] M. Mattson et al. [SELEX Collaboration], Phys. Rev. Lett. 89, 112001 (2002).
- [2] R. Aaij et al. [LHCb Collaboration], Phys. Rev. Lett. 119, 112001 (2017), [arXiv:1707.01621].
- [3] R. Aaij et al. [LHCb Collaboration], Chin. Phys. C 44, 022001 (2020), [arXiv:1910.11316].
- [4] R. Aaij et al. [LHCb Collaboration], Phys. Rev. Lett. 121, 162002 (2018), [arXiv:1807.01919].
- [5] P. A. Zyla, et al. [Particle Data Group], Prog. Theor. Exp. Phys. 083C01 (2020).
- [6] R. Aaij, et al. [LHCb Collaboration], Journal of High Energy Physics volume 95 (2020), [arXiv:2009.02481].
- [7] R. Aaij, et al. [LHCb Collaboration], Chin. Phys. C 45, 093002(2021), [arXiv:2104.04759].
- [8] [LHCb Collaboration], [arXiv:2204.09541].
- [9] A. Ali, A. Y. Parkhomenko, Q. Qin, W. Wang, Physics Letters B 782(10), 412-420 (2018), arXiv:1805.02535 [hep-ph].
- [10] A. Ali, Q. Qin, W. Wang, Physics Letters B 785(10), 605-609 (2018), arXiv:1806.09288 [hep-ph].
- [11] Z. Ghalenovi, C. P. Shen, M. M. Sorkhi, Physics Letters B 834(10), 137405 (2022), [arXiv:2204.02938].
- [12] J. T. Castellà, EPJ Web Conf. 258, 04003 (2022), [arXiv:2111.09783].
- [13] H. Z. Tong and H. S. Li, Commun. Theor. Phys. 74, 085201 (2022), [arXiv:2110.01380].

- [14] W. X. Zhang, H. Xu, and D. J. Jia, Phys. Rev. D104, 114011 (2021), [arXiv:2109.07040].
- [15] J. Soto, J. T. Castellà, Phys. Rev. D 104, 074027 (2021), [arXiv:2108.00496].
- [16] Z. G. Wang, Eur. Phys. J. C 78, 826 (2018), arXiv:1808.09820 [hep-ph].
- [17] T. M. Aliev, S. Bilimis, Nuclear Physics A 984, 99-111 (2019), [arXiv:1904.11279].
- [18] C. Y. Wang, C. Meng, Y. Q. Ma, K. T. Chao, Phys. Rev. D 99, 014018 (2019), [arXiv:1708.04563].
- [19] Q. Li, C. H. Chang, S. X. Qin, G. L. Wang, Chinese Physics C 44, 013102 (2020), [arXiv:1903.02282].
- [20] Q. X. Yu, X. H. Guo, Nuclear Physics B 947, 114727 (2019), [arXiv:1810.00437].
- [21] Q. F. Lü, K. L. Wang, L. Y. Xiao, and X. H. Zhong, Phys. Rev. D 96, 114006 (2017), arXiv:1708.04468 [hep-ph].
- [22] Z. Shah and A. K. Rai, Eur. Phys. J. C 77, 129 (2017), arXiv:1702.02726 [hep-ph].
- [23] Zalak Shah, Kaushal Thakkar, Ajay Kumar Rai, Eur. Phys. J. C 76, 530(2016), [arXiv:1609.03030].
- [24] A. Kakadiya, C. Menapara, A. K. Rai,[arXiv:2204.13438].
- [25] H. Garcilazo, A. Valcarce, J. Vijande, Phys. Rev. D94, 074003 (2016), [arXiv:1609.06886].
- [26] Y. L. Ma, M. Harada, Physics Letters B Volume 748(2),463-466 (2015), [arXiv:1503.05373].
- [27] K. W. Wei, B. Chen, N. Liu, Q. Q. Wang, X. H. Guo, Phys. Rev. D 95, 116005 (2017), arXiv:1609.02512v1 [hep-ph].
- [28] D. Ebert, R. N. Faustov, V. O. Galkin, A. P. Martynenko, Phys. Rev. D 66, 014008(2002), arXiv:hep-ph/0201217.
- [29] B. Chen, S. Q. Luo, K. W. Wei, X. Liu, Phys. Rev. D 105, 074014 (2022), [arXiv:2201.05728].
- [30] T. Yoshida, E. Hiyama, A. Hosaka, M. Oka, and K. Sadato, Phys. Rev. D 92, 114029 (2015), arXiv:1510.01067 [hep-ph].
- [31] G. L. Yu, Z. Y. Li, Z. G. Wang, J. Lu, M. Yan, [arXiv:2206.08128].
- [32] Z. Y. Li, G. L. Yu, Z. G. Wang, J. Z. Gu, J. Lu, [arXiv:2207.04167].
- [33] S. Godfrey and N. Isgur, Phys. Rev. D 32, 189 (1985).
- [34] S. Capstick and N.Isgur, Phys. Rev. D 34, 2809 (1986).
- [35] E. Hiyama, Y. Kino, and M. Kamimura, Prog. Part. Nucl. Phys. 51, 223 (2003).
- [36] J. Oudichhya, K. Gandhi, A. K. Rai, Phys. Rev. D 104, 114027 (2021), [arXiv:2111.00236].
- [37] S. Z. Shi, J. X. Zhao, and P. F. Zhuang, Chin. Phys. C 44, 084101 (2020), arXiv:1905.10627[nucl-th].
- [38] P. Mohanta and S. Basak, Phys. Rev. D 101, 094503 (2020), arXiv:1911.03741[hep-lat].
- [39] X. Z. Weng, X. L. Chen, and W. Z. Deng, Phys. Rev. D 97, 054008 (2018).
- [40] M. Karliner and J. L. Rosner, Phys. Rev. D 97, 094006 (2018), arXiv:1803.01657 [hep-ph].
- [41] T. Burch, [arXiv:1502.00675].
- [42] Z. Ghalenovi, A. A. Rajabi, S. X. Qin, D. H. Rischke, Mod. Phys. Lett. A 29, 1450106 (2014), arXiv:1403.4582 [hep-ph].
- [43] Z. S. Brown, W. Detmold, S. Meinel, and K. Orginos, Phys. Rev. D 90, 094507 (2014).
- [44] M. Karliner and J. L. Rosner, Phys. Rev. D 90, 094007 (2014), [arXiv:1408.5877].
- [45] B. Eakins and W. Roberts, Int. J. Mod. Phys. A 27, 1250039 (2012), arXiv:1201.4885 [nucl-th].
- [46] L. Tang, X. H. Yuan, C. F. Qiao, and X. Q. Li, Commun. Theor. Phys. 57, 435 (2012).
- [47] M. H. Weng, X. H. Guo, and A. W. Thomas, Phys. Rev. D 83, 056006 (2011), arXiv:1012.0082 [hep-ph].
- [48] Z. G. Wang, Eur. Phys. J. A 47, 267 (2010); Eur. Phys. J. C 68, 459 (2010).

- [49] F. Giannuzzi, Phys. Rev. D 79, 094002 (2009), arXiv:0902.4624 [hep-ph].
- [50] D. Ebert, R. N. Faustov, V. O. Galkin and A. P. Martynenko, Phys. Rev. D 70, 014018 (2004) [erratum: Phys. Rev. D 77, 079903 (2008)], arXiv:hep-ph/0404280 [hep-ph].
- [51] A. Valcarce, H. Garcilazo, and J. Vijande, Eur. Phys. J. A 37, 217 (2008).
- [52] W. Roberts and M. Pervin, Int. J. Mod. Phys. A 23, 2817 (2008), arXiv:0711.2492 [nucl-th].
- [53] A. P. Martynenko, Phys. Lett. B 663, 317 (2008), arXiv:0708.2033 [hep-ph].
- [54] J. R. Zhang and M. Q. Huang, Phys. Rev. D 78, 094007 (2008), arXiv:0810.5396 [hep-ph].
- [55] A. Bernotas and V. Simonis, Mixing of heavy baryons in the bag model calculations, Lith. J. Phys. Tech. Sci. 48, 127 (2008), arXiv:0801.3570 [hep-ph].
- [56] C. Albertus, E. Hernandez, J. Nieves and J. M. Verde-Velasco, Eur. Phys. J. A 32, 183-199 (2007) [erratum: Eur. Phys. J. A 36, 119 (2008)], arXiv:hep-ph/0610030 [hep-ph].
- [57] D. H. He, K. Qian, Y. B. Ding, X. Q. Li, and P. N. Shen, Phys. Rev. D 70, 094004 (2004), [arXiv:hep-ph/0403301].
- [58] V. V. Kiselev, A. K. Likhoded, O. N. Pakhomova, and V. A. Saleev, Phys. Rev. D 66, 034030 (2002), arXiv:hep-ph/0206140 [hep-ph].
- [59] S. S. Gershtein, V. V. Kiselev, A. K. Likhoded, and A. I. Onishchenko, Phys. Rev. D 62, 054021 (2000).
- [60] D. Ebert, R. N. Faustov, V. O. Galkin, A. P. Martynenko, and V. A. Saleev, Z. Phys. C 76, 111 (1997), arXiv:hep-ph/9607314.
- [61] B. Silvestre-Brac, Prog. Part. Nucl. Phys. 36, 263-273 (1996).
- [62] R. Roncaglia, D. B. Lichtenberg, and E. Predazzi, Phys. Rev. D 52, 1722 (1995), arXiv:hep-ph/9502251.
- [63] V. V. Kiselev, A. V. Berezhnoy, A. K. Likhoded, Phys. Atom. Nucl. 81(3), 369-372 (2018); Yad. Fiz. 81(3), 356-359 (2018), [arXiv:1706.09181].
- [64] T. Regge, Nuovo Cim. 14, 951 (1959).
- [65] T. Regge, Nuovo Cim. 18, 947-956 (1960).
- [66] G. F. Chew and S. C. Frautschi, Phys. Rev. Lett. 7, 394-397 (1961) .
- [67] G. F. Chew and S. C. Frautschi, Phys. Rev. Lett. 8, 41-44 (1962).